MRC/UVRI and LSHTM Uganda Research Unit

Medical Research Council

Uganda Virus Research Institute

LONDON SCHOOL of HYGIENE &TROPICAL MEDICINE

University of Essex

University of Sunderland

NIH National Institutes of Health
Turning Discovery Into Health

MRC/UVRI & LSHTM Uganda Research Unit, Entebbe, Uganda
Alex.Mutebe@lshtm.ac.uk

Deep Learning for Automated Detection of Periportal Fibrosis in Ultrasound Imaging: Improving Diagnostic Accuracy in Schistosoma Mansoni Infection

Alex Mutebe[1,2], Bakhtiyar Ahmed[2], Agnes Natukunda[1], Simon Mpooya[3], Emily Webb[1], Andrew Abaasa[1], Ayoub Kakande[1], Alison M. Elliott[1], Samuel O. Danso[4]

[1]Medical Research Council/Uganda Virus Research Institute and London School of Hygiene & Tropical Medicine Uganda Research Unit, Entebbe, Uganda,
[2]University of Essex, Colchester, UK, [3]Division of Vector Borne and Neglected Tropical Diseases, Ministry of Health, Uganda,
[4]School of Computer Science and Engineering, University of Sunderland, UK

Introduction

Understanding Periportal Fibrosis

- *Schistosoma mansoni* infection can lead to periportal fibrosis (PPF), a form of liver scarring around the portal tracts that significantly impacts morbidity and mortality.
- Early detection is crucial for timely intervention and potential reversibility.
- In Uganda, nearly 70% of the population residing near water bodies are affected.

Diagnostic Challenge

- Traditional ultrasound imaging, while widely used, is highly operator-dependent and requires considerable expertise for accurate diagnosis.

Objective

- This study aims to apply AI-base deep learning methods to improve liver disease diagnosis from ultrasound images.

Figure 1. US image with heterogeneous liver architecture, decreased portal vein wall definition with a positive PPF diagnosis (Nigo et al., 2021).

Methods

- **Data Source**: Liver ultrasound image dataset from a case-control study conducted by the Uganda Schistosomiasis Multidisciplinary Research Collaboration (U-SMRC).
- **Sample**: A subset of 200 ultrasound images from a total of 371, evenly distributed between cases and controls.
- Images were labelled using the Niamey protocol, with a pattern score of ≥2 indicating the presence of PPF.

Data Extraction

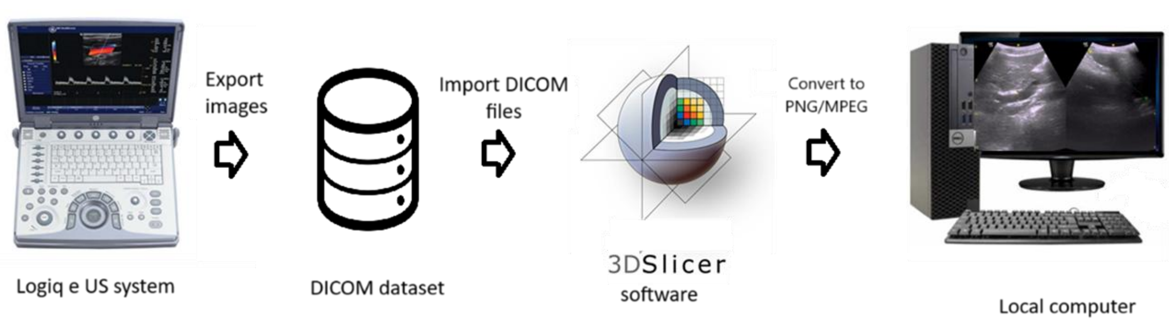

Figure 2. Pipeline illustrating the extraction and storage of ultrasonography (US) images using 3DSlicer software.

Data Pre-processing

1) Data Anonymization & Labelling
- PNG format, metadata removed
- Study IDs → anonymized

2) Image Acquisition
- Supine scans performed after fasting
- Imaging device: GE Logiq E
- Technologist with over 20 years of experience

3) Data Augmentation
- Random rotations
- Shifting
- Flips

4) Normalization
- Pixel values were converted to 32-bit floating-point format
- Mean and standard deviation statistics were used

Model Architecture

VGG16-Inspired CNN Architecture

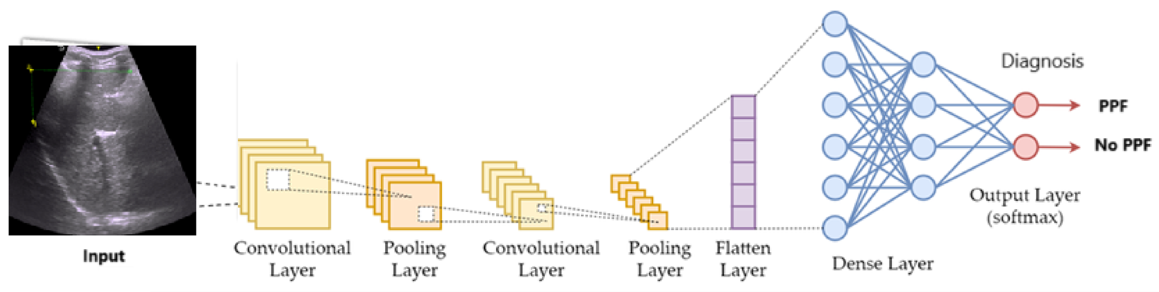

1) Model Choice & Structure

- Balance of performance & efficiency
- Captures detailed ultrasound features
- Suitable for small datasets

Model Training

- **Dataset split:** Training set(80%), Test set(20%)
- **Reproducibility**: A random seed was set in Python for reproducibility
- **Input resolution**: 32×32 images performed better than 128×128

Results

Table 1. Characteristics of study participants stratified by PPF status (N = 200).

Characteristic	No PPF (N = 100)	PPF (N = 100)
Sex		
Female	28 (28%)	18 (18%)
Male	72 (72%)	82 (82%)
Age (years)	29 (25, 37)	30 (24, 39)
Left Liver Lobe Length (cm)	6.90 (6.15, 7.60)	8.15 (7.25, 9.20)
Right Liver Lobe Length (cm)	9.90 (9.40, 10.30)	10.40 (9.90, 11.40)
Inner-to-Inner Diameter of Branch 1 (mm)	2.20 (1.80, 2.50)	2.50 (1.85, 3.10)
Outer-to-Outer Diameter of Branch 1 (mm)	4.30 (3.60, 5.10)	6.50 (5.40, 7.90)
Inner-to-Inner Diameter of Branch 2 (mm)	2.20 (1.80, 2.50)	2.50 (2.20, 3.00)
Outer-to-Outer Diameter of Branch 2 (mm)	4.00 (3.60, 4.85)	6.95 (5.45, 8.10)
Image Pattern Score		
0	88 (88%)	0 (0%)
1	12 (12%)	0 (0%)
2	0 (0%)	54 (54%)
4	0 (0%)	40 (40%)
6	0 (0%)	6 (6.0%)

Values are presented as n (%) for categorical variables and Median (Q1, Q3) for continuous variables.

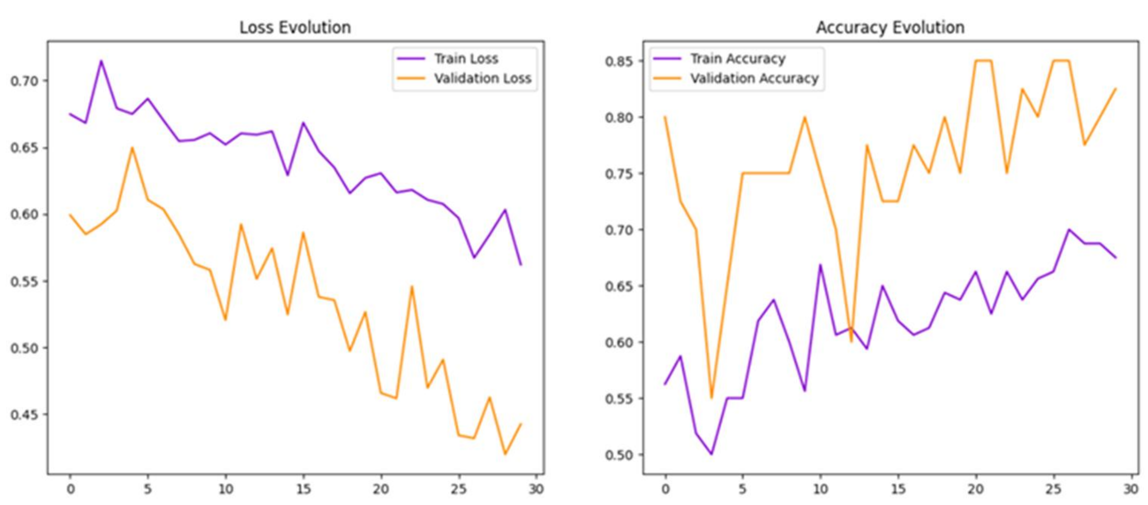

Figure 3. Despite mild oscillations, the learning curves indicated more consistent performance on unseen data.

Results

Accuracy	AUC	Precision	Sensitivity	Specificity	F1 score
80	87	76	80	76	80

Table 2: Comparison of model performance metrics

- **Test Accuracy**: 80% (95% CI: 77.5–97.5%)
- **AUC**: 0.89 (95% CI: 78–99.5%)

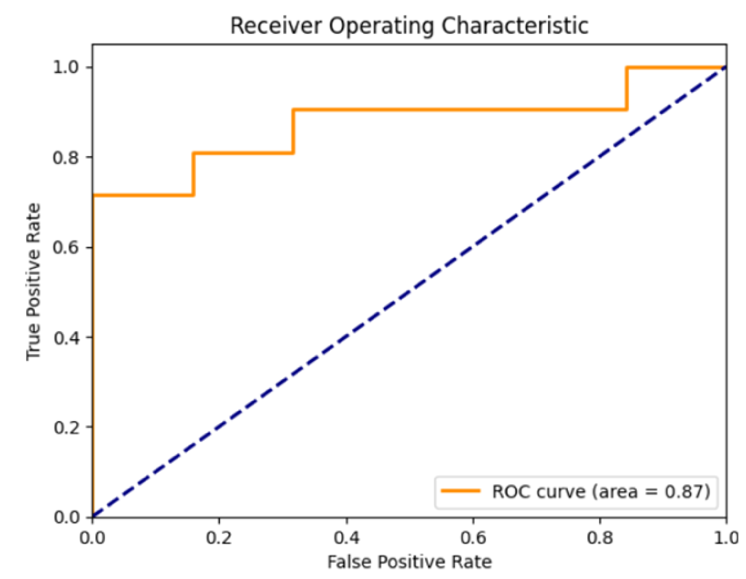

Figure 4. ROC curve, with an AUC of 0.87, demonstrating strong discriminatory ability between classes.

Discussion

- The CNN accurately detected PPF from ultrasound images, even at low resolution, while preserving key features.
- Optimised model shows high precision and balanced sensitivity, supporting early fibrosis detection.
- Pre-processing and aspect ratio preservation improve efficiency and focus on relevant structures.
- Small dataset and single-reviewer labelling are limitations.

Conclusion

The CNN model effectively detected PPF from ultrasound images, demonstrating strong diagnostic potential. AI can support standardised and accessible diagnosis in schistosomiasis-endemic regions. Future work will expand datasets, include fibrosis severity, and assess alternative architectures.

Acknowledgements

This work was supported in part by grant number 403U01AI168609 from the United States National Institute of Allergy and Infectious Diseases

References

Gunda, D. W.; Kilonzo, S. B.; Manyiri, P. M.; Peck, R. N.; Mazigo, H. D. Morbidity and mortality due to *Schistosoma mansoni* 412related periportal fibrosis: could early diagnosis of varices improve the outcome following available treatment modalities in sub 413Saharan Africa? A scoping review. Tropical Medicine and Infectious Disease 2020, 5, 20. 414

LeCun, Y., Bengio, Y., and Hinton, G. (2015). Deep learning. Nature, 521(7553), 436–444. 491

Lee, J.-G.; Jun, S.; Cho, Y.-W.; Lee, H.; Kim, G. B.; Seo, J. B.; Kim, N. Deep learning in medical imaging: general overview. Korean 429Journal of Radiology 2017, 18(4), 570–584.

Tang, X. The role of artificial intelligence in medical imaging research. BJR Open 2019, 2(1), 20190031.